Research Paper
International Journal of Aerospace System Engineering
Vol.5, No.1, pp.1-8 (2018)

ISSN 2383-4986
EISSN 2508-7169
https://doi.org/10.20910/IJASE.2018.5.1.1

Influence of Impact from Anti-Aircraft Bullet on Rotorcraft Fuel Tank Assembly

Sung Chan Kim[1], Hyun Gi Kim[1†]

Korea Aerospace Research Institute,
KOREA
†E-mail: shotgun1@kari.re.kr

Abstract

Military rotorcrafts are constantly exposed to risk from bullet impacts because they operate in a battle environment. Because bullet impact damage can be deadly to crews, the fuel tanks of military rotorcraft must be designed taking extreme situations into account. Fuel tank design factors to be considered include the internal fluid pressure, the structural stress on the part impacted, and the kinetic energy of bullet strikes. Verification testing using real objects is the best way to obtain these design data effectively, but this imposes substantial burdens due to the huge cost and necessity for long-term preparation. The use of various numerical simulation tests at an early design stage can reduce the risk of trial-and-error and improve the prediction of performance. The present study was an investigation of the effects of bullet impacts on a fuel tank assembly using numerical simulation based on SPH (smoothed particle hydrodynamics), and conducted using the commercial package, LS-DYNA. The resulting equivalent stress, internal pressure, and kinetic energy of the bullet were examined in detail to evaluate the possible use of this numerical method to obtain configuration design data for the fuel tank assembly.

Key Words : Fuel Tank; FSI(Fluid Structure Interaction); LS-DYNA; SPH(Smoothed particle hydrodynamics)

1. Introduction

The basic function of an aircraft fuel tank is to store fuel. However, fuel tank characteristics have a significant influence on the survivability of crews in aircraft emergency situations. Thus, the fuel tank should be designed by considering predictable extreme situations, such as an internal explosion or fire, in order to improve the survivability of the crew. To prove the soundness of fuel tanks, the U.S. government has established a military specification (MIL-DTL-27422) [1], and requires that relevant tests be performed under strict standards. In order to prove the soundness of a fuel tank, the preferred method is to carry out the verification test using the actual product. However, a verification test using actual products requires considerable expense. In addition, the design and manufacturing of a fuel tank takes a long time and the cost of manufacturing an experimental fuel tank may be a burden. When the fuel tank test results in failure, the cost and time for further refinement will affect the overall aircraft production period. For instance, the best-known rotorcrafts, including the AH-64 Apache, UH-60 Blackhawk utility helicopter, and tilt rotor V-22 Osprey, were all developed through several test failures and tough refinement processes [2].

For these reasons, performing a variety of numerical analyses of the fuel tank prior to proof testing could minimize the reliance on trial and error, and thereby, the overall cost. Furthermore, important design information may be produced through cooperative research, because such numerical analyses can accumulate test data over extended operating times. However, in the past there have been numerous limitations to conducting such complicated simulations, such as fluid-structure interactions (FSI), because they require significant amounts of computer resources. Recently, with advanced technological breakthroughs and

Received: Aug. 29, 2017 Revised: Dec. 13, 2017
Accepted: Dec. 13, 2017
† Corresponding Author
Tel: +82-42-870-3531, E-mail: shotgun1@kari.re.kr

developments in computing and specialized software, it has become more feasible to conduct research such as FSI using a variety of scenarios.

In this study, numerical analysis was carried out on the FSI problem of the fuel tank assembly considering the situation in which a projectile hits a military rotary wing aircraft. There are two kinds of methods for solving the FSI problem: the ALE method based on FEM, and the element free method, such as smoothed particle hydrodynamics (SPH).

With ALE, a Lagrangian mesh is set up for the structure and an Eulerian mesh for the fluid. This method can provide accurate results because it interchanges the interface information between the structure and fluid. However, it requires excessive computing time and computer resources. Moreover, under high-level impact conditions, ALE is liable to fail in a contact situation due to excessive deformation of meshes. Furthermore, it can cause fluid to leak out of the interface. SPH is based on the Lagrangian methodology. SPH assumes that each particle represents a material property within in a specific domain. Even though SPH requires a large number of particles for detailed fluid simulations, it can solve the FSI problem quickly compared to the ALE method. Regardless of twisted or excessive deformations, fluid does not leak out of the interface so long as the contact conditions at the interface are well set up. After considering the efficiency of the computing cost and propriety of the numerical simulations, this study employed the SPH method for the FSI analysis. The focus of this study was an FSI simulation based on SPH involving a bullet impact of a rotorcraft fuel tank assembly, using the commercial package LS-DYNA.

When a fuel tank is penetrated by anti-aircraft fire, there may be an internal explosion due to the sudden rise of internal fluid pressure. Moreover, once the bullet is inside the fluid, because the bullet moves irregularly, it is possible that it may have a fatal effect on the condition of the fuel tank itself and internal attachments. Empirically, the bullet is likely to puncture the exit portion in the inclined posture. When the bullet hits with high kinetic energy, it may also endanger the survival of the aircraft and crew by causing excessive fuel leakage. In view of these emergency situations, in this present study, critical design information such as the behavior of the bullet, the internal fluid pressure, and the stress values were estimated. Furthermore, by evaluating how changes in the kinetic energy of the bullet affect the fuel tank, we were able to assess the potential for acquiring design data that could help prepare for bullet impact situations.

In this study, we considered the real time dynamic behavior of the fuel tank assembly and the internal fluid under a bullet impact load using an explicit method. The equivalent stress was calculated for each fuel tank and the weak areas of each fuel tank assembly were investigated under bullet impact loads.

In this paper, Section 2 introduces the SPH methodology. Section 3 explains the conditions of the numerical simulation, including the material information and analysis models using FEM and SPH. Finally, Section 4 presents the results of the numerical simulation of the bullet impact on the fuel tank assembly.

2. Review of Smoothed Particle Hydrodynamics

SPH represents large deformations well because it does not have fixed connectivity between particles. This method can easily be applied to complex geometries and large-scale features are easy to obtain by tracing the particle motions. Because of these advantages, SPH has been primarily applied for shock simulations, free surface flows, and sound propagation [3-7]. Recently, it has been effectively applied to high explosive simulations and high velocity impact computations [8-10].

The field values of each particle, $\langle f(x) \rangle$ are evaluated using the smoothing kernel function. The SPH formation is presented in Eq. (1), as follows:

$$\langle f(x) \rangle = \int_{\Omega} f(x') W(x - x', h) dx' = \sum_{j=1}^{N} \frac{m_j}{\rho_j} f(x_j) W(x - x_j, h) \quad (1)$$

Here, ρ is the particle density, m is the particle mass, h is the smoothing length, and $\langle f(x_j) \rangle$ is the physical value at the j position.

$W(x)$ is the smoothing kernel function, in which a cubic spline function is mainly used. $W(x)$ should satisfy the three kinds of condition presented in Eq. (2) to Eq. (4).

Normalization condition : $\int_{\Omega} W(x - x', h) dx' = 1$ (2)

Delta function property : $\lim_{h \to 0} W(x - x', h) = \delta(x - x')$ (3)

Compact condition : $W(x - x', h) = 0$ when $|x - x'| > \kappa h$ (4)

In Eq. (4), κ is a constant value that defines the effective non-zero area in the smoothing kernel function.

In SPH, the continuity equation, momentum equation, and energy conservation are discretized as described in Eq. (5) to (7). The equations are evaluated at each time step using the explicit integration procedure [11-12].

Continuity equation: $\frac{d\rho_i}{dt} = \sum_j m_j (v_i - v_j) \nabla_i W_{ij}$ (5)

Momentum equation : $\frac{dv_i}{dt} = -\sum_j m_j \left(\frac{p_j}{\rho_i^2} + \frac{p_i}{\rho_j^2} \right) \nabla_i W_{ij}$ (6)

Energy conservation : $\frac{du_i}{dt} = \frac{1}{2}\sum_j m_j \left(\frac{p_j}{\rho_i^2} + \frac{p_i}{\rho_j^2} \right) v_{ij} \nabla_i W_{ij}$ (7)

Here, ∇_i is a Laplacian operator.

However, SPH has a defect in shock problems: therefore, it uses artificial viscosity to improve its shock capturing abilities. The artificial viscosity functions as a resistive pressure and thermalizes the kinetic energy in the shock by converting it to thermal energy. Then, this artificial viscosity term is added to the momentum and energy equations as given in Eq. (8) and Eq. (9).

Momentum with artificial viscosity :

$$\frac{dv_i}{dt} = -\sum_j m_j \left(\frac{p_j}{\rho_i^2} + \frac{p_i}{\rho_j^2} + \Pi_{ij} \right) \nabla_i W_{ij} \quad (8)$$

Energy with artificial viscosity :

$$\frac{du_i}{dt} = \frac{1}{2}\sum_j m_j \left(\frac{p_j}{\rho_i^2} + \frac{p_i}{\rho_j^2} + \Pi_{ij} \right) v_{ij} \nabla_i W_{ij} \quad (9)$$

where, artificial viscosity

$$\Pi_{ij} = \begin{cases} \dfrac{-\alpha \hat{c}_{ij} \mu_{ij} + \beta \mu_{ij}^2}{\rho_{ij}} & v_{ij} \cdot \gamma_{ij} < 0,\ \mu_{ij} = \left(h v_{ij} \cdot \gamma_{ij} \right) / \left(\gamma_{ij}^2 + \eta^2 \right) \\ 0 & v_{ij} \cdot \gamma_{ij} > 0 \end{cases}$$

$\hat{c}_{ij}$ is the mean sound speed at position i and j.

3. Conditions for Numerical Analysis

3.1. Material of Fuel Tank

As seen in Fig. 1, the fuel tank material largely consists of three layers. The reinforcing layer supports the external load. In detail, the nylon 66 molded into the rubber determines the stiffness value of the reinforcing layer. The layer of self-sealing material is located between the reinforcing layers. It repairs damaged areas by swelling of its sponge structure after being punctured.

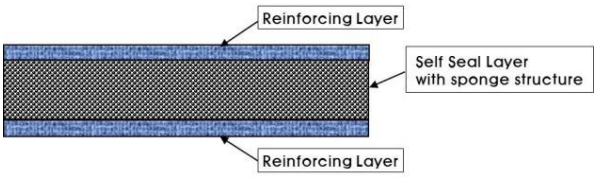

Fig. 1 Section of the Fuel Tank Material

3.2. Numerical Model and Condition for Analysis

The overall configuration of the fuel tank assembly is presented in Fig. 2. The names of each fuel tank component and other critical components (such as metal fittings) are given in the figures. The fuel tank assembly consists of four components: forward fuel tank (FFT), first feeder tank (FT1), after fuel tank (AFT), second feeder tank (FT2). The FFT and AFT store fuel; the FT1 and FT2 transfer the fuel into the engine through the booster pump. Thus, the FT1 and FT2 are called feeder tanks.

The numerical model consisted of a bulkhead, fuel tank assembly, and plumbing. Each fuel tank consisted of a metal fitting and skin. The Mooney-Rivlin material model was employed for the fuel tank skin and the material data was acquired from previous research [13]. The metal fittings are mainly used to install the line replacement unit (LRU) or attach the fuel tank to the fuselage. As provided in Table 1, the material of the bulkhead, metal fitting, and plumbing is aluminum. The thicknesses of the bulkhead and plumbing were 2.0 *mm*; the metal fitting was 10.0 *mm*, and the skin was 10.0 *mm*. The diameter of the bullet was 20 *mm* and its material type was assumed to be a rigid body with cylindrical configuration. The velocity of a normal bullet is 900-1000 *m/s*. This study sets the initial bullet speed to 650 *m/s* by assuming the conditions of striking a rotorcraft from 800 *m* away. Two directions of impact, straight in and diagonal, were considered.

The total number of shell elements for the fuel tank assembly was 68,641. In detail, the FFT was constructed with 21,200 shell elements and the AFT had 15,541 shell elements. The FT1 had 10,005 shell elements and FT2 had 10,003 shell elements. The bulkhead was represented by 16,165 shell elements. As shown in Fig.3, the internal fluid was filled to 85% of the volume of each fuel tank with total particles of 1,207,614. To ensure the results of the FSI analysis, the contact conditions between the structure and fluid had to be well defined. In this study, the contact keywords applied, were provided in LS-DYNA (e.g., single surface, node-to-surface, and surface-to-surface). All contact conditions between each part are given in Table 2.

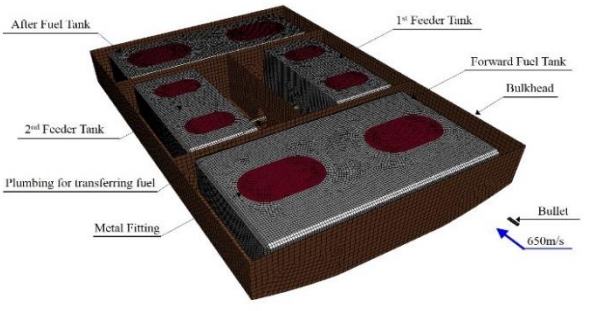

Fig. 2 Numerical Simulation Model of Fuel Tank Assembly

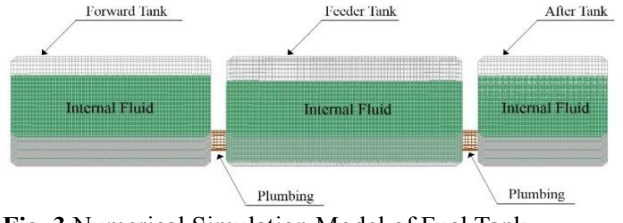

Fig. 3 Numerical Simulation Model of Fuel Tank Assembly

Table 1 Materials Properties for Data Input

Part	Input Data
Fluid	▪ Density : 998 kg/m^3
Skin of fuel tank	▪ Material model : Mooney-Rivlin Material ▪ Density : 980 kg/m^3 ▪ Poisson ratio : 0.49 ▪ Thickness : 10mm
Metal fitting, Bulkhead Plumbing	▪ Material model: Piecewise linear plasticity ▪ Density : 2,867 kg/m^3 ▪ Young's modulus : 72.4GPa ▪ Poisson ratio : 0.33 ▪ Thickness $\begin{cases} metal\ \ fitting : 10mm \\ bulkhead,\ plumbing : 2mm \end{cases}$
Bullet	▪ Material model : Rigid ▪ Density : 17,000 kg/m^3 ▪ Young's modulus : 370GPa ▪ Poisson ratio : 0.17 ▪ Diameter : 14.5mm ▪ Initial speed : 650m/s

Table 2 Contact Conditions for Numerical Simulation of Crash Impact

Contact condition	Applied Part
Single Surface	▪ fuel tank group ▪ bulkhead
Node to Surface	▪ fuel tank group ↔ fluid particle ▪ plumbing ↔ fluid particle ▪ bulkhead ↔ fluid particle ▪ bullet ↔ fluid particle
Surface to Surface	▪ bulkhead ↔ fuel tank group ▪ bulkhead ↔ bullet ▪ fuel tank group ↔ bullet

4. Results of Numerical Analysis

Numerical simulation was performed for impacts to the front of the fuel tank assembly from straight and diagonal approaches. Analysis time was 0–0.015 s and the time step was 6.69×10^{-7} s. Simulation took about 48 h with 64 bit computers.

4.1. Impact on the Front of the Fuel Tank Assembly after Straight Approach

4.1.1 Internal Behavior, Pressure and Energy

Fig. 4 shows the behavior of the internal fluid after the bullet impact to the front of the fuel tank assembly from a straight approach. After being discharged toward the side of the FFT, the bullet penetrates the bulkhead, FFT, and FT1 progressively. In this process, significant damage is produced at the exit area of the FFT and entry area of the FT1 by the tumbling bullet. The damaged areas at the FFT exit and FT1 entry are shown in Fig. 5.

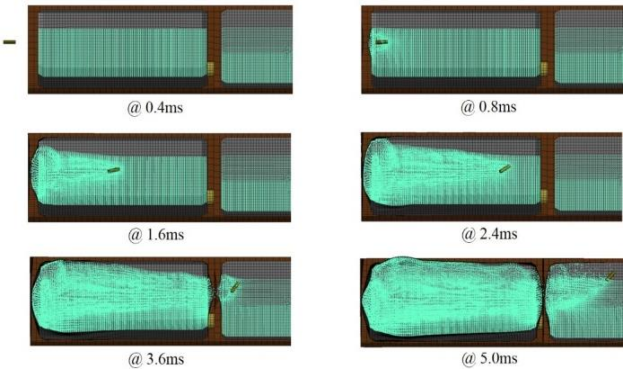

Fig. 4 Behavior of Internal Fluid and Bullet (Section View)

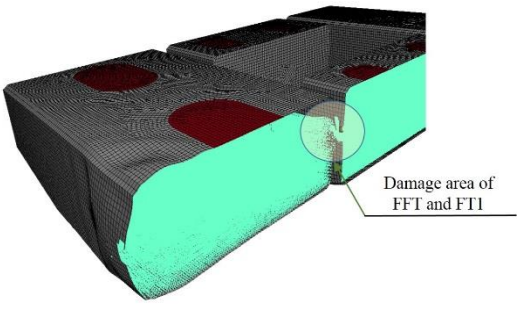

Fig. 5 Damage of FFT Exit Area and FT1 Entry Area

Fig. 6 and 7 show the maximum pressure in the FFT and FT1. The maximum pressure was calculated to be 103.0 *MPa* and 67.6 *MPa* in the FFT and FT1, respectively.

In Fig. 6, the internal pressure of the FFT jumps at 1.0 *ms*, then, is reduced more than 80% after 2.0 *ms* due to the sudden loss of kinetic energy. Because that bullet goes through the bulkhead and FFT, the maximum pressure in the FT1 was calculated to be 67.6 *MPa*, which is a relatively small value compared to that in the FFT because of the great amount of energy lost by penetration of the bulkhead and FT1, as shown in Fig. 7

Fig. 8 shows the change in kinetic energy of the bullet over time. At the initial stage of impact, its kinetic energy is calculated to be 76,500 *J*. When the bullet impacts the FT1 after penetrating the FFT and bulkhead, its kinetic energy has been reduced by 87% (calculated to be about 10,100 *J*). Finally, the kinetic energy of the projectile is reduced to 4840 *J* (at 6.6 *ms*) after going through the FT1 interior.

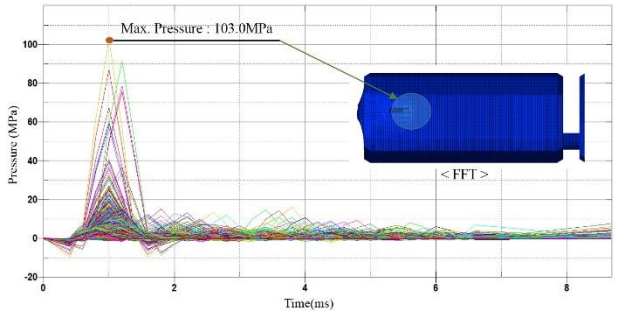

Fig. 6 Internal Pressure in FFT(Max. at1.0ms)

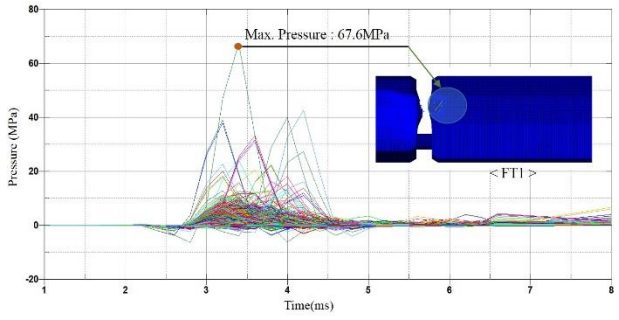

Fig. 7 Internal Pressure in FT1(Max.at 3.4ms)

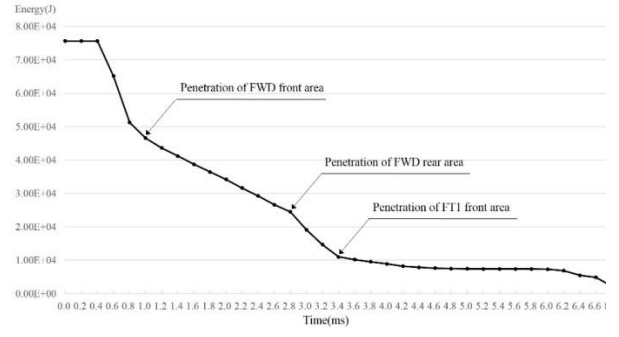

Fig. 8 Kinetic Energy of Bullet

4.1.2 Estimation of Equivalent Stress

Fig. 9 is the stress contour of the fuel tank assembly when the maximum equivalent stress occurs. The maximum equivalent stress (300.1 *MPa*) is produced on the upper metal fitting of the FFT. It is generated at the time that the bullet goes through the FT1 after completely penetrating the FFT.

The internal behavior of the fluid at that moment is shown in Fig. 10. When the bullet initially penetrates the FFT, the internal fluid is pushed upward suddenly. Because this behavior results in a bending effect, the maximum stress occurs on the upper metal fitting. The material of the metal fitting is Aluminum 2014 T6. Considering a tension strength of 485 *MPa* (yield strength 415 *MPa*), it is estimated that the metal fitting has a safety factor of 1.3 times.

Fig. 11 and 12 show the distribution of the equivalent stress on the plumbing and the fuel tank skin with the exception of the area directly damaged by the bullet. The maximum stress value of the plumbing that connects the FFT and the FT1 is 93.2 *MPa* at 6.0 *ms*. In Fig. 12, the maximum equivalent stress of the fuel tank skin is 49.9 *MPa* at 2.2 *ms*. From the results of a specimen test in a previous study, the damage strength of the skin material was measured to be 144.89 *MPa* [13]. Thus, it can be estimated that the skin area of the fuel tank has a safety factor of more than twice.

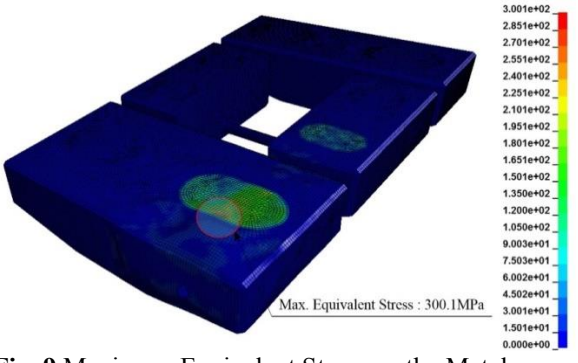

Fig. 9 Maximum Equivalent Stress on the Metal Fitting

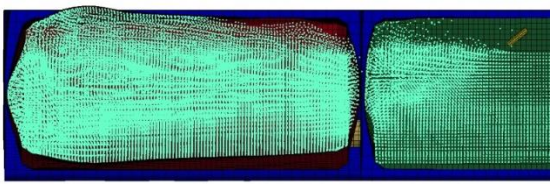

Fig. 10 Behavior of Internal Fluid at the Critical Time

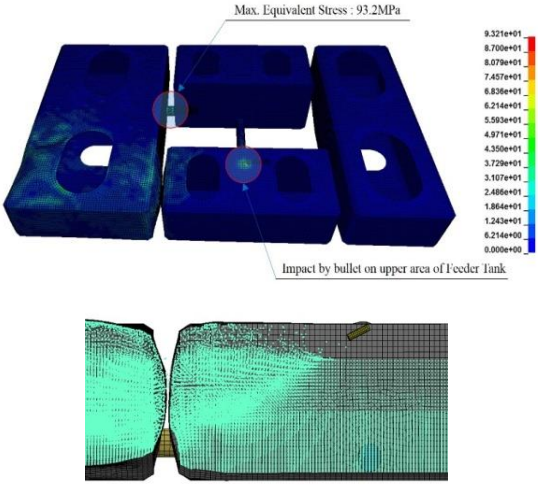

Fig. 11 Maximum Equivalent Stress on the Plumbing and Behavior of Internal Fluid at 6.0ms

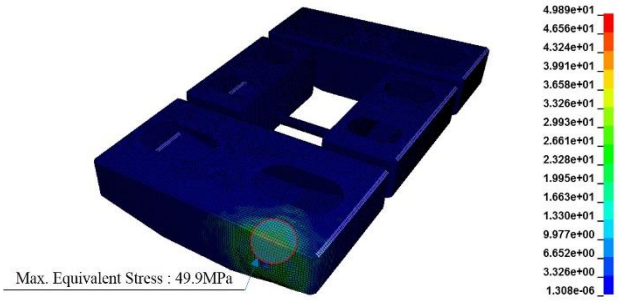

Fig. 12 Maximum Equivalent Stress on the Skin at 2.2ms

4.2. Impact to Front of the Fuel Tank Assembly after Diagonal Approach

Fig. 13–14 presents the behavior of the internal fluid and the bullet when the bullet impacts the FFT after a diagonal approach (45°). It can be seen that the bullet is tumbled by the fluid resistance while passing through the FFT, and that the tumbling bullet causes serious damage at the exit area. The damage to the exit area is shown in Fig. 15.

Fig. 16 shows the variation of the kinetic energy of the bullet. The initial energy (76,500 *J*) of the bullet was calculated to be reduced to about 4950 *J* after passing through the FFT, a reduction in energy of about 94%.

Fig. 17 shows the pressure distribution of the internal fluid in the FFT of the entry and exit areas. The maximum pressure in the entry and exit areas is calculated to be 40.3 *MPa* at1.8 *ms* and 100 *MPa* at 6.6 *ms*, respectively. As shown in Fig. 18, the impact load caused by the hydraulic ram effect influences the metal fittings as a bending load. As a result, the maximum equivalent stress on the metal fittings is calculated to be 317 *MPa* (300.1 *MPa* from straight approach). The maximum equivalent stress of the plumbing connecting the FFT and FT1 is calculated to be 161.2 *MPa* (93.2 *MPa* from in straight approach). In addition, the maximum equivalent stress on the tank skin was calculated to be 51 *MPa* (49.9 *MPa* from straight approach). As a result, it is considered that the case of impact from a diagonal approach is relatively critical compared to impact from a straight approach, in terms of equivalent stress.

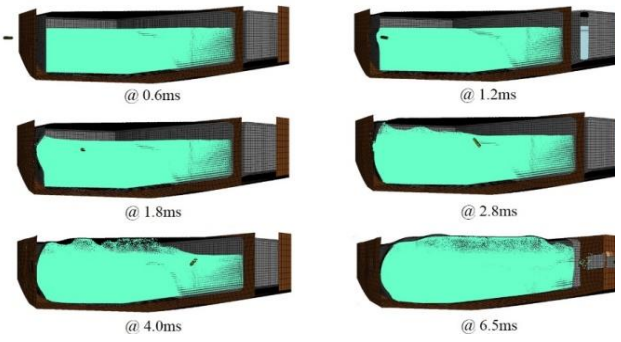

Fig. 13 Behavior of Internal Fluid &Bullet(Section View)

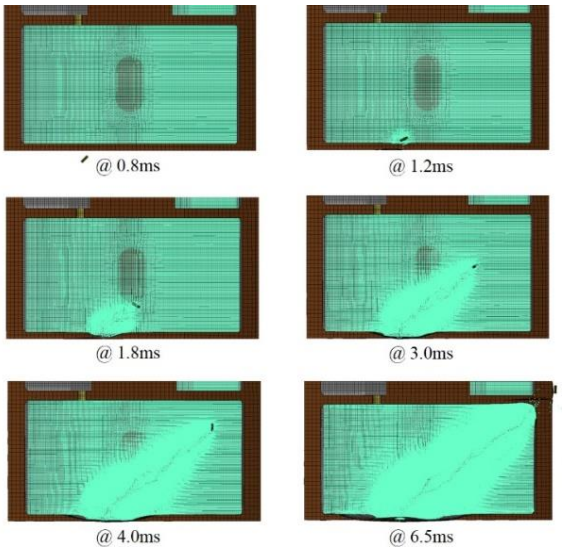

Fig. 14 Behavior of Bullet(Top view)

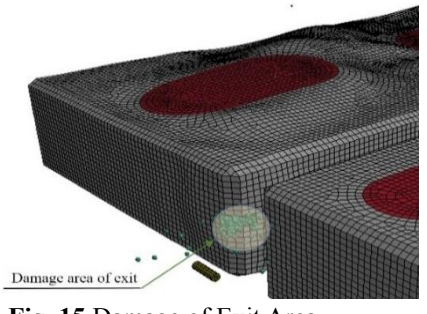

Fig. 15 Damage of Exit Area

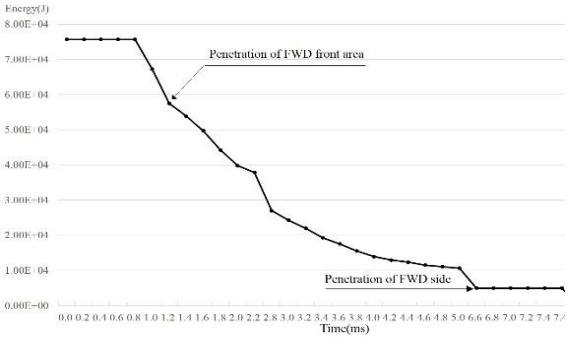

Fig. 16 Kinetic Energy of Bullet

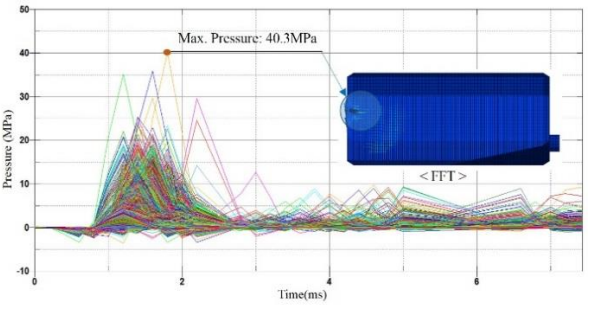

<Internal Pressure in Entry Area>

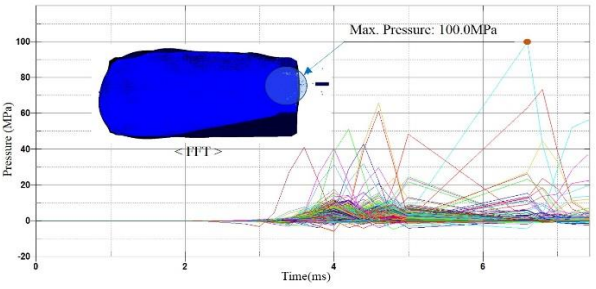

<Internal Pressure in Exit Area>

Fig. 17 Internal Pressure in Entry and Exit Area of FFT

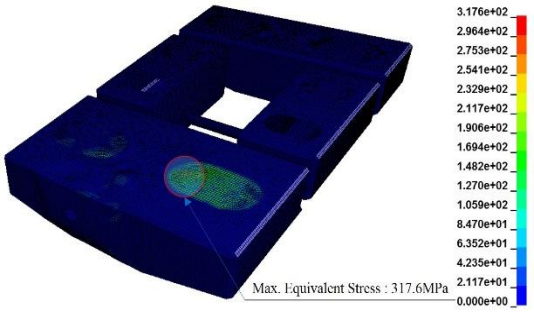

<Equivalent stress at Metal Fitting>

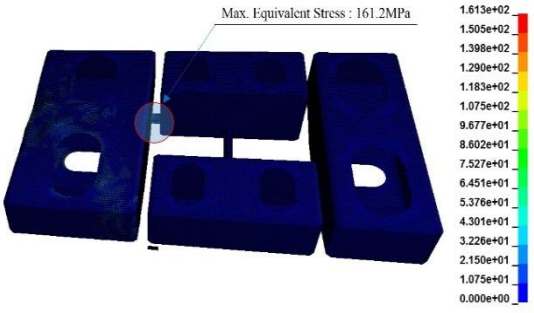

<Equivalent stress at Plumbing>

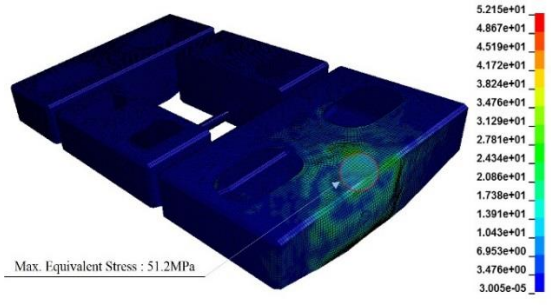

<Equivalent stress at Skin>

Fig. 18 Maximum Equivalent Stress at Metal Fitting, Plumbing and Skin

5. Conclusions

This study presented an FSI analysis based on SPH simulating bullet impacts with the fuel tank assembly. The validity of the commercial software (LS-DYNA) for the application was demonstrated using numerical examples.

The behavior of the bullet was investigated by numerical results and the fluid pressure caused by the bullet impact and trajectory was calculated. Moreover, the maximum equivalent stress value was calculated and vulnerable areas were investigated in each fuel tank.

Numerical analysis was performed for two cases, where the bullet impacted the fuel assembly perpendicular to its side (90°), and from a 45° angle. In both cases, the portion of the fuel tank where the bullet exited was severely damaged because the bullet began tumbling after penetrating the internal fluid.

In the case of straight impact (perpendicular), it was found that the maximum pressure was 103 *MPa* at the FFT entry area and 100 *MPa* from FFT exit area with diagonal impact, indicating the same maximum level of pressure. The calculated maximum equivalent stress was 300.1 *MPa* for the metal fitting, 93.2 *MPa* for plumbing, and 49.9 *MPa* for the skin after a straight impact; while for the diagonal impact, it was 317.6 *MPa* for the metal fitting, 161.2 *MPa* for the plumbing, and 51.2 *MPa* for the skin. From the analysis results, it was evaluated that diagonal impact is a relatively critical case in terms of equivalent stress. Also, it is considered that the metal fitting and the fuel tank skin have sufficient the margin of safety for the two impact conditions in this study.

This study only performed numerical simulations considering a bullet impact to the front of the fuel tank assembly, and considering only the bulkhead and fuel tanks. However, there could be much more severe cases involving a bullet impact in the fuel tank assembly. Therefore, to improve the crew's survivability, various additional critical conditions need to be considered in the design of the fuel tank assembly. This study shows that there are various design parameters that could affect the bullet resistance capability of the fuel tanks. In the future, the reliability of the numerical simulations acquired in this study should be verified and, if necessary, the data correlation approach between the numerical simulation and actual test should be conducted. Moreover, this study will be extended to include estimations of bullet impact to a full-scale airframe coupled with an internal LRU and surrounding components

Acknowledgement

This study was carried out with the support of the Aerospace Component Technology Development Project of the Ministry of Trade, Industry and Energy.

References

[1] U.S. Army Aviation and Missile Command, “Detail Specification for the Tank, Fuel, Crash-Resistant, Ballistic-Tolerant, Aircraft”, MIL-DTL-27422D, 2007.

[2] Ugone, Mary L., Meling, John E., Snider, Jack D., Gause, Neal J., Carey, Alice F., “Acquisition: Fuel Tanks of the V-22 Osprey Joint Advanced Vertical Aircraft”, D-2003-013, 2002.

[3] Monaghan, J., Gingold, R., “Shock simulation by the particle method SPH”, *Journal of Computational Physics*, vol. 52, no. 2, pp.374-389, 1983.

[4] Monaghan, J., “Smoothed particle hydrodynamics”, *Annual Review of Astronomy and Astrophysics,* vol. 30, pp.543-574, 1992.

[5] Herreros, M.I., Mabssout, M., “A two-steps time discretization scheme using the SPH method for shock wave propagation”, *Computer Methods in Applied Mechanics and Engineering*, vol. 200, pp. 1833–1845, 2011.

[6] Shao, J.R., Li, H.Q, Liu, G.R., Liu, M.B., “An improved sph method for modeling liquid sloshing dynamics”, *Computers and Structures*, vol. 100-101, pp.18-26, 2012.

[7] Jean-Christophe Marongiu, Francis Leboeuf, JoËlle Caro, Etienne Parkinson, “Free surface flows simulations in pelton turbines using a hybrid SPH-ALE method”, *Journal of Hydraulic Research.*, vol. 48, no. 1, pp. 40-49, 2010.

[8] Liu, M., Liu, G., Zong, Z., Lam, K., “Computer simulation of high explosive explosion using smoothed particle hydrodynamics methodology”, *Computers and Fluids*, vol. 32, no. 3, pp.305-322, 2003.

[9] Liu, M., Feng, D.L., Guo, Z.M., “Recent developments of SPH in modeling explosion and impact problems”, *International Conference on Particle-based Methods-Fundamentals and Applications*, Stuttgart, Germany, September, 2013.

[10] Johnson, G., Stryk, R., Beissel, S., “SPH for high velocity impact computations”, *Computer Methods in Applied Mechanics and Engineering*, vol. 139, pp. 347-373, 1996.

[11] Hahn, Philipp, “On the use of meshless methods in acoustic simulations”, Thesis of Master, University of Wisconsin, Madison, WI, 2009

[12] Naval Surface Weapons Center, “Prediction of Impact Pressures, Forces, and Moments during Vertical and Oblique Water Enter”, NSWC/WOL/TR77-16, 1997.

[13] Kim, Hyun-Gi, Kim, Sung Chan, “Numerical simulation of crash impact test for fuel tank group of rotorcraft”, *International Journal of Crashworthiness*, vol. 19, no. 6, pp. 639-652, 2014.